

Improved Prediction of Lateral Deformations due to Installation of Soil-Cement Columns

Jinchun Chai¹; John P. Carter²; Norihiko Miura³; and Hehua Zhu⁴

Abstract: A modified method is proposed for predicting the lateral displacements of the ground caused by installation of soil-cement columns. The method is a combination of the original method derived on the basis of the theory of cylindrical cavity expansion in an infinite medium and a correction function introduced to consider the effect of the limited length of the columns. The correction function has been developed by comparing the solutions obtained using the spherical and the cylindrical cavity expansion theories for a single column installation. Both the original and the modified methods have been applied to a case history reported in the literature, which involves clay soils, and the predictions are compared with field measurements. The advantage of the modified method over the original method is demonstrated. Finally, the modified method has also been applied to a case history involving loose sandy ground, and the calculations show that the method can also be used for this type of soil provided that appropriate consideration is given to the volumetric strain occurring in the plastic zone of soil surrounding the soil-cement columns.

DOI: 10.1061/(ASCE)GT.1943-5606.0000155

CE Database subject headings: Cement; Mixing; Lateral displacement; Cavitation; Soil stabilization; Columns; Installation.

Introduction

Mixing cement with clayey soil in the ground (deep mixing), normally forming soil-cement columns in situ, is a widely used soft ground improvement method. During soil-cement column installation, either cement slurry (wet mixing) or cement powder (dry mixing) is injected into the ground under pressure and application of this pressure will cause deformation of the surrounding subsoil. In an urban environment, this deformation may be very significant because it can affect existing nearby structures. Therefore, predicting and controlling the lateral displacements induced by soil-cement column installation are important design considerations.

Chai et al. (2005, 2007) proposed a method to predict the lateral displacement caused by soil-cement column installation based on the theory of an infinitely long cylindrical cavity expansion in an infinite soil medium. Successful application of the method to four case histories in Saga, Japan was demonstrated. However, actual soil-cement columns have limited length, and the method generally overpredicts the lateral displacement near the ends of the columns. For cases where the columns extend to the

ground surface this overprediction is most pronounced near the base of the column and for cases where columns are installed only within a soil sublayer it occurs near both the top and bottom of the column. Close to the ends of these columns the confining effects of the soil layers below and/or above the columns tend to reduce the induced lateral displacement. However, the original method proposed by Chai et al. (2005, 2007) does not consider these effects. There are many cases in practice where these columns are installed within a soil sublayer and they do not extend to the ground surface, e.g., in cases where soil beneath the base of an excavation is improved prior to excavation.

In this paper a correction function is proposed to consider the effect of the finite length of the installed column. Combination of the original method proposed by Chai et al. (2005, 2007) and the correction function forms the modified method. In the following sections the method proposed by Chai et al. (2005, 2007) is briefly reviewed, and the development of the correction function is explained. Finally, application of both the original and the modified methods to case histories in clay soils and sandy ground is presented.

Brief Review of the Original Method

The method proposed by Chai et al. (2005, 2007) is based on the theory of cylindrical cavity expansion in an infinite medium proposed by Vesic (1972). Vesic presented solutions for both a cylindrical and a spherical cavity expansion in a linear elastic-perfect plastic soil of infinite extent that obeys the Mohr-Coulomb failure criterion. It is noted that since Vesic presented his approach, more sophisticated cavity expansion theories have been proposed, such as those that consider strain hardening/softening behavior of soil (e.g., Prevost and Hoeg 1975); theories considering soil consolidation (e.g., Carter 1988); those considering dilatancy behavior of soil (e.g., Yu and Houlsby 1991); and theories using critical state constitutive soil models (e.g., Collins and Yu 1996). However, the soil media considered here are soft clays and

¹Professor, Dept. of Civil Engineering, Saga Univ., 1 Honjo, Saga 840-8502, Japan (corresponding author). E-mail: chai@cc.saga-u.ac.jp

²Pro Vice-Chancellor, Faculty of Engineering and Built Environment, The Univ. of Newcastle, New South Wales 2308, Australia. E-mail: john.carter@newcastle.edu.au

³Principal, Institute of Soft Soil Engineering, Co., Ltd., Saga 840-0811, Japan. E-mail: miuran@viola.ocn.ne.jp

⁴Professor, School of Civil Engineering, Tongji Univ., 1239 Siping Rd., Shanghai 200092, China. E-mail: zhuhhk@online.sh.cn

Note. This manuscript was submitted on October 11, 2007; approved on May 14, 2009; published online on May 23, 2009. Discussion period open until May 1, 2010; separate discussions must be submitted for individual papers. This paper is part of the *Journal of Geotechnical and Geoenvironmental Engineering*, Vol. 135, No. 12, December 1, 2009. ©ASCE, ISSN 1090-0241/2009/12-1836-1845/\$25.00.

Table 1. Equations for Calculating Lateral Displacements Caused by Cylindrical and Spherical Cavity Expansion

Equation number	Item	Cylindrical (a)	Spherical (b)	Reference
Eq. (1)	Radius of plastic zone, R_p	$\frac{R_p}{R_u} = \sqrt{I_r},$ $I_r = \frac{E}{2(1+\nu)S_u} = \frac{G}{S_u}$	$\frac{R_p}{R_u} = \sqrt[3]{I_r},$ $I_r = \frac{E}{2(1+\nu)S_u} = \frac{G}{S_u}$	
Eq. (2)	Limiting cavity pressure, p_u	$p_u = S_u \cdot F_c + p_0 \cdot F_q,$ $F_q = 1.0$ $F_c = \ln(I_r) + 1 \quad (2a)$	$p_u = S_u \cdot F_c + p_0 \cdot F_q,$ $F_q = 1.0$ $F_c = \frac{4}{3}[\ln(I_r) + 1] \quad (2b)$	Vesic (1972)
Eq. (3)	Pressure at $r=R_p$, σ_p	$\sigma_p = p_u - 2S_u \ln\left(\frac{R_p}{R_u}\right)$	$\sigma_p = p_u - 4S_u \ln\left(\frac{R_p}{R_u}\right)$	
Eq. (4)	Displacement at $r=R_p$, δ_p	$\delta_p = \frac{1+\nu}{E} R_p (\sigma_p - p_0) = \frac{1+\nu}{E} R_p S_u$	$\delta_p = \frac{1+\nu}{2E} R_p (\sigma_p - p_0) = \frac{2(1+\nu)}{3E} R_p S_u$	Chai et al. (2005, 2007) for cylindrical case. Equations for spherical case have been derived in this study.
Eq. (5)	Displacement in plastic zone, δ ($R_u \leq r \leq R_p$)	$\delta \approx \frac{2R_p + \delta_p}{2r + \delta_p R_p / r} \delta_p$	$\delta = \frac{1}{R_p^2/R_u^2 - 1} \left[\frac{R_p^2}{R_u^2} \delta_p - \delta_u + (\delta_u - \delta_p) \frac{R_p^2}{r^2} \right]$	
Eq. (6)	Displacement in elastic zone, δ ($r \geq R_p$)	$\delta = \frac{R_p}{r} \delta_p = \frac{R_u^2}{2r}$	$\delta = \frac{R_p^2}{r^2} \delta_p = \frac{R_u^3}{3r^2}$	

Note: R_u =the radius of a cavity; δ_u =displacement at R_u ; r =radius from the center of a cavity; E =Young's modulus of the soil; G =shear modulus of the soil; S_u =undrained shear strength of the soil; ν =Poisson's ratio of the soil; p_0 =initial mean stress in the ground; F_c , F_q =cavity expansion factors; and I_r =rigidity index.

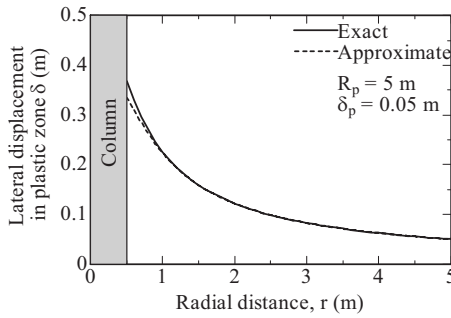


Fig. 1. Comparing the calculated lateral displacement in the plastic zone

saturated loose sandy deposits, and the loading process is close to the undrained condition for clays or may be partially drained in the case of loose sandy deposits, so that ignoring dilatancy as well as strain hardening or softening should not induce much error, provided appropriate parameter values are selected to characterize the behavior of the ground. Hence, for simplicity, the solutions given originally by Vesic (1972) are adopted in the present study.

Following the theory proposed by Vesic, equations for calculating the lateral displacement induced by these cavity expansions are summarized in Table 1. They are numbered as Eqs. (1a) and (1b) to Eqs. (6a) and (6b) for the specific case of an undrained soil for which the friction angle, $\phi=0$, and for which volumetric strain in the plastic zone, $\Delta=0$. It is worth noting that Eq. (5a) is not a rigorous expression. A precise expression can be obtained by solving a quadratic equation, but in order to obtain an explicit equation for the lateral displacement caused by installing a row of columns, an approximation form [Eq. (5a)] has been adopted. Further Eq. (5a) has been derived by using initial values of the parameters R_u , R_p , and r , so that for cases involving large displacements, there will be some error involved. The magnitude of the errors depends on the values of r , R_p , and δ_p . The smaller the value of r and the larger the values of R_p and δ_p , the larger the error. For the cases reported by Chai et al. (2005), R_p is in a range from about 1.5 to 5 m, and δ_p from about 0.015 to 0.05 m [the larger values are for the wet jet mixing (WJM) method]. Using $R_p=5.0$ m, $\delta_p=0.05$ m, and $r \geq 0.5$ m, Fig. 1 compares the calculated lateral displacement in the plastic zone. It can be seen that the maximum error is about 9%. It is noted that Eq. (5b) is also

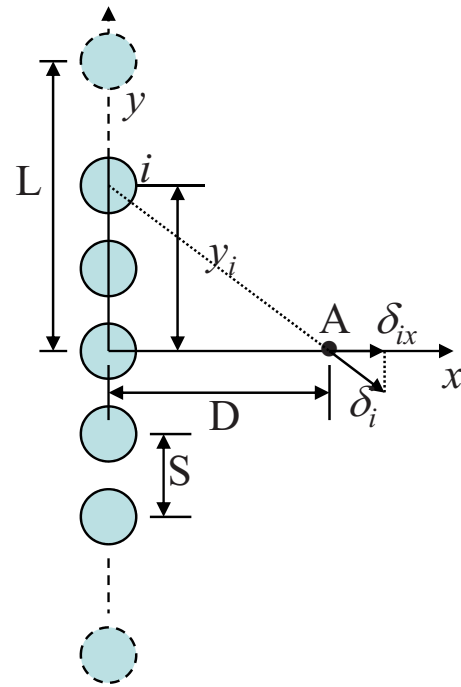


Fig. 2. Plan section illustration of the lateral displacement in the x -direction caused by installation of a single row of soil-cement columns

derived using initial values of the parameters R_u , R_p , and r , but it is a rigorous expression.

The additional equations numbered as Eqs. (7)–(9), which are based on the application of the theory of cylindrical cavity expansion, may be used to calculate the lateral displacement at Point A in the x -direction caused by installing a single row of the soil-cement columns in clayey soil (Fig. 2). These equations are listed in Table 2 (Chai et al. 2007). In deriving the equations in Table 2, the method of superposition has been adopted. Strictly speaking, superposition is applicable for linear elastic materials only. The soil model assumed in the analysis is linear elastic-perfectly plastic, and so using superposition in the plastic zone will also induce some error (possibly a slight overprediction of the lateral displacements). It is also noted that the method of superposition has

Table 2. Equations for Calculating Lateral Displacement Caused Installation of a Single Row of Columns

Equation number	Condition	Lateral displacement
Eq. (7)	For $D < R_p$ and $D^2 + L^2 > R_p^2$	$\delta_{xA} = \frac{2D(2R_p + \delta_p)\delta_p}{S\sqrt{4D^2 + 2R_p\delta_p}} \tan^{-1} \sqrt{\frac{2(R_p^2 - D^2)}{2D^2 + R_p\delta_p}}$ $+ \frac{2R_p\delta_p}{S} \left(\tan^{-1} \frac{L}{D} - \tan^{-1} \sqrt{\frac{R_p^2}{D^2} - 1} \right)$
Eq. (8)	$D < R_p$ and $D^2 + L^2 \leq R_p^2$	$\delta_{xA} = \frac{2D(2R_p + \delta_p)\delta_p}{S\sqrt{4D^2 + 2R_p\delta_p}} \tan^{-1} \sqrt{\frac{2L^2}{2D^2 + R_p\delta_p}}$
Eq. (9)	For $D \geq R_p$	$\delta_{xA} = \frac{2R_p\delta_p}{S} \left(\tan^{-1} \frac{L}{D} \right)$

Note: D =offset distance from the center of a row of columns to the point of interest; S =spacing between two adjacent columns in a row; and L =half length of a row. Equations in this table assume that the point of interest is on the perpendicular bisector of a row of columns. If the point of interest is not on the bisector of the row, two calculations are needed, i.e., using two different values of L and then averaging the results.

been used to consider the effect of an installation composed of multiple rows of soil-cement columns.

It can be seen from the governing equations that in addition to the geometric conditions, the parameters controlling the lateral displacement are R_p and δ_p . Both R_p and δ_p are functions of I_r and R_u [Eqs. (1) and (4) in Table 1]. The rigidity index, I_r , is a basic soil parameter, being a measure of the soil's stiffness to strength ratio. R_u , the radius of a cavity, is also a crucial parameter controlling the amount of lateral displacement that will occur. The installation of a soil-cement column is neither a displacement controlled nor a pressure controlled process. It is a process of injecting a predetermined amount of cement slurry/powder into the ground by predetermined pressures (which may not be precisely controlled). For example, injecting the same amount of admixture into the ground by the cement deep mixing (CDM) method and by the WJM method, which normally uses a higher injection pressure, will in general cause different lateral displacements. Therefore, several factors will affect the value of R_u . The first of these is the injection pressure (p) of the admixture and the second is the effective volume of admixture injected into the subsoil per unit length of a column (Δvol), which in some cases may include the amount of water injected into the ground prior to injecting the admixture. The effective volume means the total volume injected into the ground, which is obtained after subtracting the volume of returned spoil (slurry and clay mixture). The third and fourth factors affecting the value of R_u are the undrained shear strength (S_u) and the modulus (E) of the subsoil. At present, there are insufficient data available to derive a meaningful theoretical expression for R_u in terms of all these factors. Instead, empirical equations have been proposed to evaluate R_u (Chai et al. 2005).

The effect of the injection pressure p is incorporated indirectly in the back-fitted radius of the cavity, R_{u0} , which also depends on the amount of injected admixture and the soil conditions (specifically the modulus E_0). An empirical equation has been proposed to consider the effects of S_u and E on R_u . Since for most soft clayey deposits, E can be estimated as a linear function of S_u , only E is required as a variable in this empirical expression, and consequently the following simple power function has been selected

$$R_u = R_{u0} \left(\frac{E_0}{E} \right)^{1/3} \quad (10)$$

where R_{u0} =radius of the cavity corresponding to a modulus of E_0 .

There are three main methods used for soil-cement column installation in Japan, namely, the CDM method, the dry jet mixing (DJM) method, and the WJM method. The cement slurry double mixing (SDM) method reported by Chai et al. (2005) is one of the CDM methods. The injection pressures used in these methods are usually different. By back-fitting the field measured data from three sites in Saga, Japan, Chai et al. (2005) proposed R_{u0} values for these three methods, as listed in Table 3, together with the corresponding values of p , Δvol , and E_0 .

For a given installation method, the effect of varying Δvol on R_{u0} can be estimated under equivalent volume conditions. Suppose the value of R_{u0} corresponding to Δvol_1 is R_{u01} , then for Δvol_2 , the corresponding value R_{u02} can be approximated as

$$R_{u02} = R_{u01} - \frac{\Delta vol_1 - \Delta vol_2}{2\pi R_{u01}} \quad (11)$$

Development of a Correction Function

The correction function is developed by comparing the solution based on the theory of a spherical cavity expansion with that of a cylindrical cavity expansion for a single column installation. The original method (Chai et al. 2005, 2007) is based on the theory of an infinitely long cylindrical cavity expansion in an infinite medium. Specifically, it is not a half-space solution, which implies that the method does not satisfy the stress conditions at the free surface and it ignores the vertical displacement of the free surface during soil-cement column installation. Considering the simplicity of the resulting equations [Eqs. (7)–(9) in Table 2] and the fact that one of the key parameters, R_u , is determined empirically, this violation of the free surface boundary condition has been accepted as a reasonable approximation.

However, when simulating the installation of a column of limited length as a series of spherical cavity expansions, the effect of the free surface has to be considered. The theoretical solution for the expansion of a single spherical cavity in a half-space has been presented by Keer et al. (1998). For the case of a series of spherical cavity expansions an approximate solution can be obtained, at least in principle, by adopting the method of superposition. In practice it is difficult to obtain an explicit closed form solution for this case because of difficulties with the required integration. For simplicity, it is proposed to take into account the effect of the free surface in an approximate manner by using a virtual image approach, as shown in Fig. 3. Using the theory of spherical cavity expansion in an infinite space implies that there is an infinitely thick soil layer existing above the ground surface, which will restrain the lateral displacement induced by the spherical cavity expansion. In reality, no such restraint exists. Therefore, the main propose of using the virtual imagine approach is to eliminate this “virtual restriction” on lateral displacement. The lateral displacements caused by the expansion of both the real and the imaginary spherical cavities in an infinite space are superposed. In this case, the condition of zero shear stress at the free surface is not strictly satisfied, and zero vertical displacement at the free surface is imposed, but this approximate approach is at least consistent with the original method.

As shown in Fig. 3, it is assumed that a soil-cement column is formed by a series of spherical cavity expansions with a spacing of S_s along a straight line. The lateral displacement at Point A in the x -direction δ_{ix} caused by the i th and the im th spherical cavity expansions can be calculated as follows:

$$\delta_{ix} = \delta_i \frac{D_r}{\sqrt{D_r^2 + z_i^2}} + \delta_{im} \frac{D_r}{\sqrt{D_r^2 + z_{im}^2}} \quad (12)$$

where D_r =horizontal offset (radial) distance from the center of the column to Point A; z_i and z_{im} =respectively the vertical distances between Point A and the i th spherical cavity and the corresponding im th imaginary cavity; and δ_i and δ_{im} =displacement components at Point A in the corresponding radial directions. The overall lateral displacement at Point A in the x -direction (δ_{xA}) caused by installation of a single column can then be calculated from the appropriate integration, as follows:

$$\delta_{xA} = \frac{D_r}{S_s} \int_{-H_2}^{H_1} \frac{\delta}{\sqrt{D_r^2 + z^2}} dz + \frac{D_r}{S_s} \int_{2Z_0+H_2}^{2Z_0+H_2+H} \frac{\delta}{\sqrt{D_r^2 + z^2}} dz \quad (13)$$

where S_s =center-to-center spacing of two adjacent spherical cavities in a column; H =length of the column; H_1 and H_2 =vertical distances from Point A to the bottom and the top of the column; and Z_0 =vertical distance from the ground surface to the top of the

Table 3. Back Estimated Empirical Parameters

Mixing method	Injection pressure p (MPa)	Injected volume Δvol (m^3/m)	Radius R_{u0} (m) ($E_0=2250$ kPa)
CDM	0.1–0.2	0.146	0.21
DJM	0.5–0.7	0.036	0.46
WJM	~20	0.146	0.58

column. When the radial distance $r = \sqrt{(D_r^2 + z^2)} > R_p$, δ in Eq. (13) can be calculated from the elastic solution [Eq. (6b) in Table 1], and the result of the integration is as follows:

$$\delta_{xA} = \frac{R_p^2 \delta_p}{S_s \cdot D_r} \left[\frac{H_1}{\sqrt{D_r^2 + H_1^2}} + \frac{H_2}{\sqrt{D_r^2 + H_2^2}} + \frac{2Z_0 + H_2 + H}{\sqrt{D_r^2 + (2Z_0 + H_2 + H)^2}} - \frac{2Z_0 + H_2}{\sqrt{D_r^2 + (2Z_0 + H_2)^2}} \right] \quad (14)$$

If the length of a column (H) approaches ∞ , Eq. (14) reduces to

$$\delta_{xA} = \frac{2R_p^2 \delta_p}{S_s \cdot D_r} \quad (15)$$

If it is assumed that the radii of the plastic zones (R_p) created around a cylindrical and a spherical cavity must be the same, and if the lateral displacement expressed in Eq. (15) is equated to the displacement expressed by Eq. (6a) in Table 1, and $D_r=r$, and $(\delta_p)_{spherical} = 2(\delta_p)_{cylindrical}/3$ [refer to Eqs. (4a) and (4b) in Table 1], where the subscripts spherical and cylindrical refer to the values for a spherical and a cylindrical cavity expansion, respectively, S_s can be obtained as follows:

$$S_s = \frac{4}{3} R_p \quad (16)$$

This process for obtaining S_s is illustrated in Fig. 4.

As indicated by Eq. (1) in Table 1, the ratio of the radius of the plastic zone and the cavity radius is different for cylindrical and

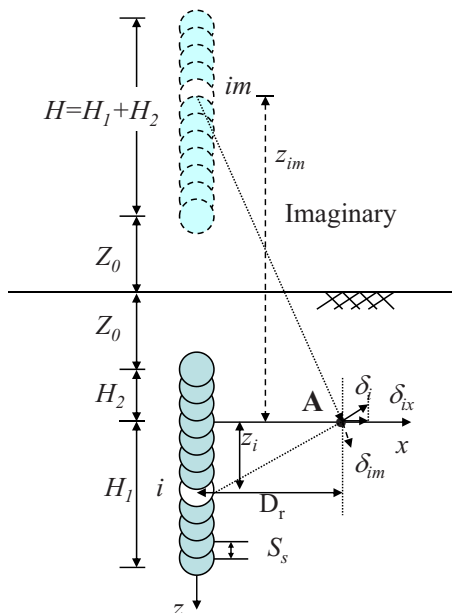


Fig. 3. Vertical section illustration of the lateral displacement in the x -direction caused by installation of a single soil-cement column

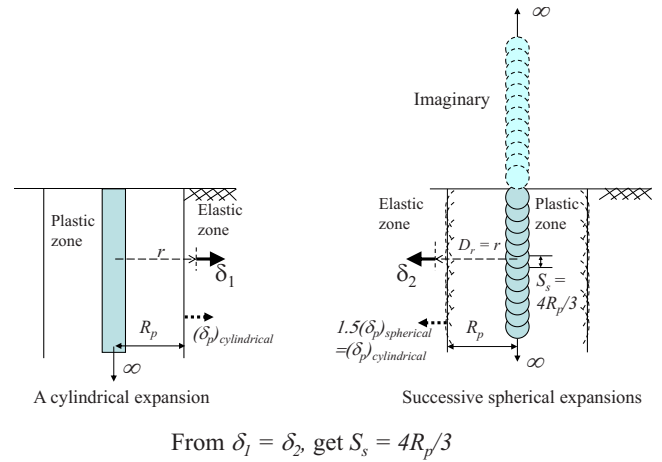


Fig. 4. Illustration of the conditions for getting the expression for S_s

spherical cavities. Assuming the same radius of the plastic zone for each case implies that the radius of the spherical cavity must be larger than the radius of the cavity in the cylindrical case. In this case the ratio of the radii of the spherical and cylindrical cavities is designated as R_{sc} , which can be expressed as a function of the rigidity index (I_r) of soil

$$R_{sc} = I_r^{1/6} \quad (17)$$

As shown in Fig. 5, R_{sc} increases with I_r , and for I_r in the range from 10 to 200, the value of R_{sc} is about 1.5 to 2.4.

If the expression for S_s given in Eq. (16) is substituted into Eq. (14) and the resulting expression for the lateral displacement is compared with Eq. (6a) in Table 1, the ratio of lateral displacement (RLD) caused by a column with limited length to that predicted by an infinitely long cylindrical cavity expansion can be evaluated, as follows:

$$RLD = \frac{1}{2} \left[\frac{H_1}{\sqrt{D_r^2 + H_1^2}} + \frac{H_2}{\sqrt{D_r^2 + H_2^2}} + \frac{2Z_0 + H_2 + H}{\sqrt{D_r^2 + (2Z_0 + H_2 + H)^2}} - \frac{2Z_0 + H_2}{\sqrt{D_r^2 + (2Z_0 + H_2)^2}} \right] \quad (18)$$

For the case of a single column, Eq. (18) indicates the effects of the horizontal offset radial distance (D_r), the length of the column (H), and the location of the point interested (Z_0, H_1, H_2) on RLD. Fig. 6 shows the variation in RLD with depth for two assumed cases at a location 5 m horizontally from the center of the column. Case 1 is a situation where the column is installed at depths between 5 and 15 m, and Case 2 is a column installed to

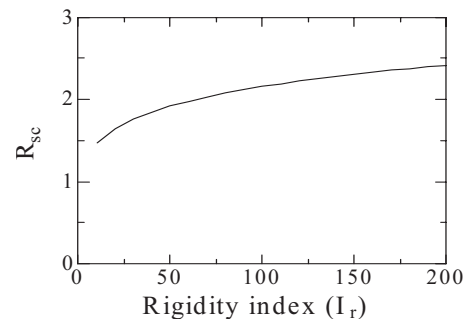


Fig. 5. Variation of R_{sc} with I_r

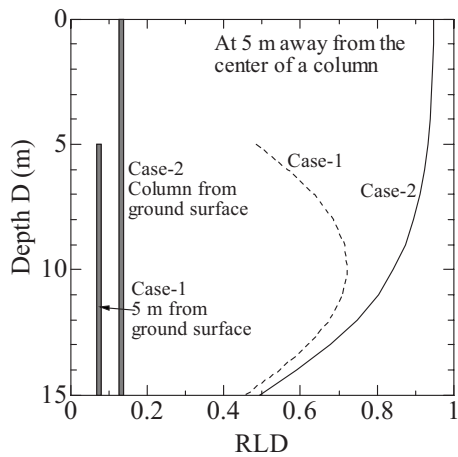


Fig. 6. Example variation of RLD with depth for a single column case

15 m depth from the ground surface. For Case 1, RLD has its largest value around the middle of the column and reduces toward the two ends, and for Case 2, RLD reduces with depth. Fig. 7 shows the variation in RLD with distance from the column for a point at the middle of the 15 m length of column assumed in Case 2. Fig. 7 shows that RLD reduces significantly with the offset (radial) distance from the column. It is noted that Eq. (18) was obtained assuming that the point of interest lies within the elastic zone of the soil around the column. Considering that Eq. (18) simply provides a geometrical correction factor, for analytical convenience it is assumed that this equation can also be used to sufficient accuracy for points located within the plastic zone.

In engineering applications, soil-cement columns are normally installed in a single row or in multiple rows. In the case of a row of columns, the offset (radial) distance from each column to the point of interest is different and Eq. (18) cannot be directly applied to the equations shown in Table 2. Using the principle of superposition, the lateral displacement induced by installing a single row of columns with limited length can be expressed as follows:

$$\delta_{xA} = \frac{2D}{S} \int_0^L \frac{\delta}{\sqrt{D^2 + y^2}} \text{RLD}(\sqrt{D^2 + y^2}) dy \quad (19)$$

where $\text{RLD}(\sqrt{D^2 + y^2})$ represents the function of Eq. (18) with the variable of $D_r = \sqrt{D^2 + y^2}$. The meanings of other parameters are

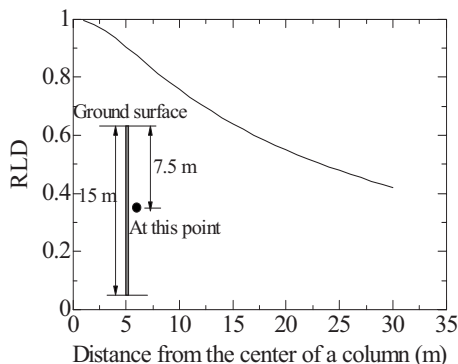


Fig. 7. Example variation of RLD with radial distance for a single column case

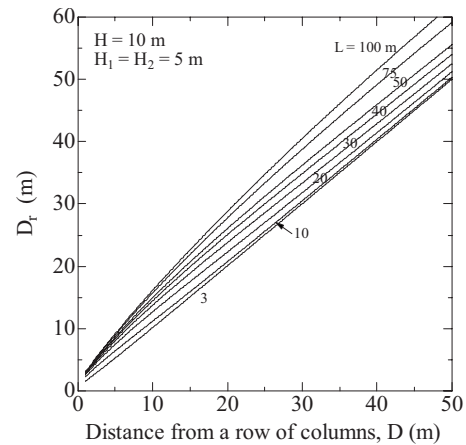


Fig. 8. Radial distance D_r as a function of D and L

indicated in Fig. 2. Integration of Eq. (19) becomes complicated and explicit forms have not been obtained. However, the integration of Eq. (19) can be easily done numerically. The values of RLD (varying with depth) for a single row of columns can be evaluated by using the numerical result of Eq. (19) and the lateral displacement calculated by the equations in Table 2 for a single row of infinite cylindrical cavity expansions. L is defined as the length from the point of interest to one end of a row. For cases where the point of interest is located on the perpendicular bisector of a row, L is half the total length of the row. For cases where the point of interest does not lie on the bisector of the row, two separate calculations with different values of L are needed, and then the results must be averaged. Numerical results indicate that the representative value of D_r in the elastic zone from the integration of Eq. (19) not only depends mainly on the values of D and L , but also on the length of the columns (H), and the location of the target point (H_1 , H_2 , and Z_o). The results given in Fig. 8 were produced using $H=10$ m, $H_1=H_2=5$ m, and $Z_o=0$. Assuming H varies from 5 to 30 m, and Z_o from 0 to 10 m, and with the D_r values given in Fig. 8, limited numerical investigation indicates that the maximum error in estimating D_r is about 15% for $D=1.0$ m, and the corresponding error on RLD is about 3%. This error reduces rapidly with increasing D (see Fig. 1).

Taken together, Eq. (18) and the representative offset (radial) distance D_r obtained from Fig. 8 form the correction function. Multiplying the correction function by the lateral displacement values obtained from Eqs. (7)–(9) (Table 2) forms the modified method for predicting the lateral displacement caused by installation of soil-cement columns in soft deposits.

Application to a Case History in Clayey Ground

Shen et al. (1999) reported a case where three field tests involving installation of soil-cement columns using the CDM, DJM, and WJM methods were conducted along the bank of the Rokkaku River in Saga, Japan. All these cases were analyzed by Chai et al. (2005). At this site soft Ariake clay is deposited with a thickness of about 15 m. The natural water contents of the soft Ariake clay are 80–120% and these values are slightly higher than the corresponding liquid limits. The undrained shear strength (S_u), derived from unconfined compression test results, is within a range of 15–30 kPa. For each installation method, three rows of columns with five columns per row were constructed under the toe of an

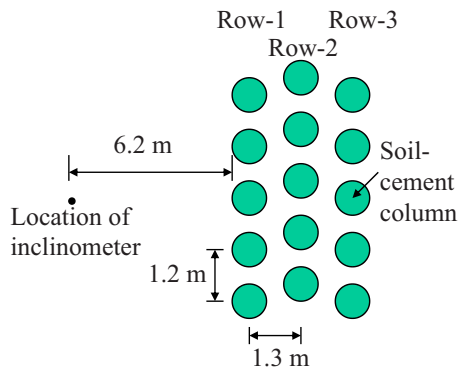


Fig. 9. Plan layout of columns and the location of inclinometer of Saga case

embankment. At the site where the DJM method was used the columns were installed from the ground surface to a depth of 13 m with a diameter of about 1.0 m. The layout of the columns and the location of inclinometer casing are illustrated in Fig. 9. For this case the lateral displacements caused by installation of each row of columns were measured, and these are compared here to the values predicted by the original and the modified methods. For this site, the ratio E/S_u of about 150 is adopted, and the back-fitted R_u value is 0.46 m, corresponding to an E value of 2250 kPa and (dry) mass injected Δvol of 0.036 m^3/m (Table 3). Other details can be found from Chai et al. (2005). $E/S_u=150$ was selected based on the reported values of the ratio E_{50}/S_u (E_{50} is the secant modulus at the stress level equivalent to 50% of peak strength) of 100–200 for soft Ariake clay (Fijikawa et al. 1996).

The predicted and the measured lateral displacements at the ground surface are compared in Fig. 10. It can be seen that the modified method predicted a faster reduction in the lateral displacement with distance from the columns and these predictions are closer to the measured data. Comparison of the variation in the lateral displacement with depth at 6.2 m from the edge of the columns is given in Fig. 11. Although both the original and the modified methods overpredicted the lateral displacements within about the top 5 m, the modified method yielded a much better prediction. Two more detailed observations can be made from Fig. 11. The first is that the modified method resulted in a much better prediction of the increments of the lateral displacement caused by installation of Rows 2 and 3 (see Fig. 9), i.e., a better prediction of the variation in the lateral displacement with distance from the column is observed for the modified method. The second observation is that the modified method predicted a smaller value of lateral displacement near the bottom of the col-

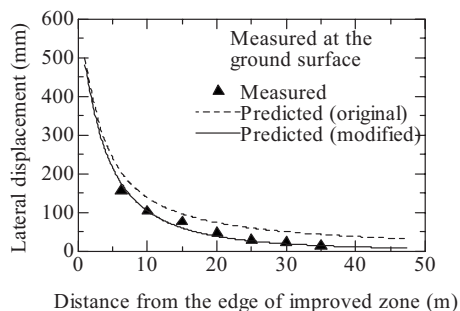


Fig. 10. Comparison of lateral displacements at the ground surface of Saga case

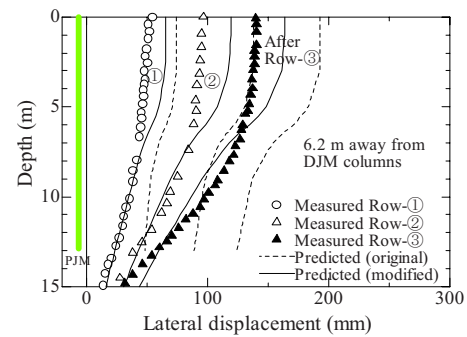


Fig. 11. Lateral displacement increments caused by each row of DJM-installed columns of Saga case

umn, which was closer to the measured data. Note that the measured surface lateral displacements given in Figs. 10 and 11 at a distance of 6.2 m from the edge of the improved zone are slightly different. The data given in Fig. 10 were measured from a surface mark and are larger than the corresponding inclinometer readings (Fig. 11).

The comparisons made above clearly demonstrated the advantage of the modified method over the original method.

Application to Case Involving Sandy Ground

Modification of Equations

The method described previously for calculating the effects of column installation was for clayey soil deposits for which the assumptions of undrained soil behavior and an internal friction angle $\phi=0$ were made. However, the method can be extended for a cohesive-frictional deposit, such as sandy ground. The main modification required relates to the equations used for calculating the lateral displacement (δ_p) at the location of the boundary between the plastic and elastic soil zones. Assuming a Mohr-Coulomb failure criterion and an effective stress approach, it is not difficult to show that the corresponding equations are as follows (rearranged from Vesic 1972).

For a cylindrical cavity expansion

$$\delta_p = \frac{1 + \nu}{E} R_p (c' \cdot \cot \phi' + p_0) \sin \phi' \quad (20a)$$

and for a spherical cavity

$$\delta_p = \frac{1 + \nu}{2E} R_p (c' \cdot \cot \phi' + p_0) \frac{4 \sin \phi'}{3 - \sin \phi'} \quad (20b)$$

The effective stress strength parameters of the soil are the cohesion, c' , and friction angle, ϕ' . With these modifications, the expression for the spherical cavity spacing, S_s [Eq. (16)], becomes

$$S_s = R_p \frac{4 \sin \phi'}{(3 - \sin \phi') \sin \phi'} \quad (21)$$

For values of ϕ' of 1° – 45° , Eq. (21) gives $S_s=(1.34-1.74)R_p$. However, the resulting expression for RLD [Eq. (18)] remains the same.

In the analysis presented previously for clay soils it was assumed that the soil behaved in an undrained manner, so that no volumetric strain would occur in the plastic zone ($\Delta=0$). However, during the injection of cement slurry into sandy ground,

some drainage can occur in the soil resulting in finite volumetric strain in the plastic zone surrounding the column. In order to consider the effect of a finite value of Δ , the reduced rigidity index (I_{rr}) should be used instead of I_r , as recommended by Vesic (1972). The relevant expressions for I_r and I_{rr} are as follows:

$$I_r = \frac{E}{2(1 + \nu)(c' + p_0 \tan \phi')} \quad (22)$$

so that for a cylindrical cavity

$$I_{rr} = \frac{I_r}{1 + I_r \Delta \sec \phi'} \quad (23a)$$

and for a spherical cavity

$$I_{rr} = \frac{I_r}{1 + I_r \Delta} \quad (23b)$$

As indicated in Eqs. (23a) and (23b), for a given value of Δ and for cases where $\phi' > 0$, the value of the reduced rigidity index I_{rr} for the cylindrical case will be smaller than for the spherical case. Conversely, a larger value of Δ would be required in the spherical case to result in the same value of reduced rigidity index for both the cylindrical and spherical cases. This latter condition is adopted when applying Eq. (18) to sandy soils.

It is also noted that Eq. (1) (in Table 1) remains the same for the spherical case but has to be changed for the cylindrical case in sandy soils, following the recommendation of Vesic (1972), i.e., in this case,

$$\frac{R_p}{R_u} = \sqrt{I_{rr} \sec \phi'} \quad (24)$$

Eq. (5) in Table 1 has been derived based on the assumption of no volumetric strain in the plastic zone. For cases where $\Delta > 0$, Eq. (5) will predict smaller lateral displacement in the plastic zone, especially near the cavity boundary. It is considered that this error has no great practical significance and therefore Eq. (5) has not been modified for the case of sandy soils.

Case History Involving Sandy Ground

Minami et al. (2007) and Sato et al. (2007) reported a case history that involved installation of soil-cement columns in loose sandy ground to form walls arranged in grids in plan-view. The purpose of these walls was to prevent potential liquefaction of the ground contained within them. The profiles of grain-size composition, natural water content, void ratio, total unit weight, and standard penetration test (SPT) N -values for this site are given in Fig. 12. The grain-size distribution curves for the samples from about 12.3 to 13.3 m depths are given in Fig. 13. Except for the SPT N -values (from Sato et al. 2007), all other data plotted in Figs. 12 and 13 are provided by Dr. E. Sato of the Takenaka Corporation, Japan. It can be seen that the D_{50} is about 0.1–0.2 mm and the sand layer is a potentially liquefiable deposit. At the site the groundwater level was about 1.0 m below the ground surface. For the sandy soil layers above 16 m depth, there are no measured data on total unit weight. Using the measured initial water contents, values of total unit weight of 17.5, 17.2, and 18.2 kN/m³ have been estimated for the soil layers from 0 to 4.5 m, 4.5 to 7.0 m, and 7.0 to 16.0 m depth, respectively.

The depth of improved soil was 16.0 m from the ground surface (as indicated in Fig. 12). The plan-view of the improved areas and the construction sequence are shown in Fig. 14 (after Minami et al. 2007). The machine used for this ground improve-

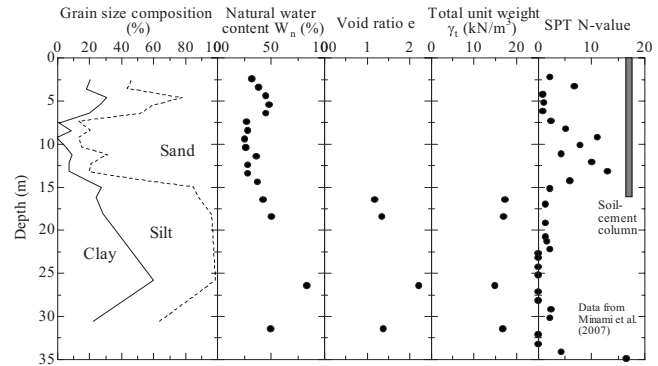


Fig. 12. Profiles of grain-size composition, natural water content, void ratio total unit weight, and SPT N -value of the sandy ground

ment project is capable of constructing two soil-cement columns of a diameter of about 1.0 m at the same time, with a center-to-center spacing of 0.8 m. The construction speed was 1.0 m/min. in the vertical direction (personal communication with Dr. E. Sato). The adjacent columns were deliberately overlapped to form a continuous wall, and the average center-to-center spacing between the adjacent columns was about 0.8 m. With different design requirements for the strengths of the columns on the perimeter and on the inside, the amount of cement injected into each type of column was different. For the pairs of columns designates as Nos. 1–17 and 31, the amount of cement used was about 2.06 kN/m³, and for column Nos. 18–30 and 32–44, it was 1.56 kN/m³. The water/cement ratio of the slurry by weight was 70% (Minami et al. 2007). Considering the unit weight of cement particles as 29.8 kN/m³, the volume of slurry injected into the ground can be evaluated as 0.216 and 0.165 m³/m³ for the cement contents of 2.06 and 1.56 kN/m³, respectively, and for a column with a diameter of 1.0 m, the corresponding volume of slurry injected for 1.0 m length will be 0.17 and 0.13 m³/m, respectively.

For the case reported by Minami et al. (2007) and Sato et al. (2007), there are no test data for the values of c' and ϕ' for the soil strata. The ϕ' values listed in Table 4 were determined from SPT N -values using the equation proposed by Japanese Railway (JSCE 1986), i.e.,

$$\phi' = 1.85^\circ \times \left(\frac{N}{0.7 + \sigma'_v/p_a} \right)^{0.6} + 26^\circ \quad (25)$$

where σ'_v = effective vertical stress and p_a = atmospheric pressure. The effective stress c' values shown in Table 4 have been determined purely empirically, based on experience. In selecting these

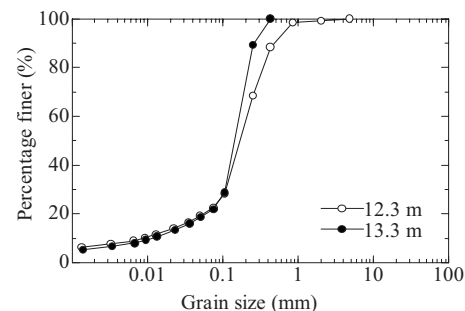


Fig. 13. Grain-size distributions

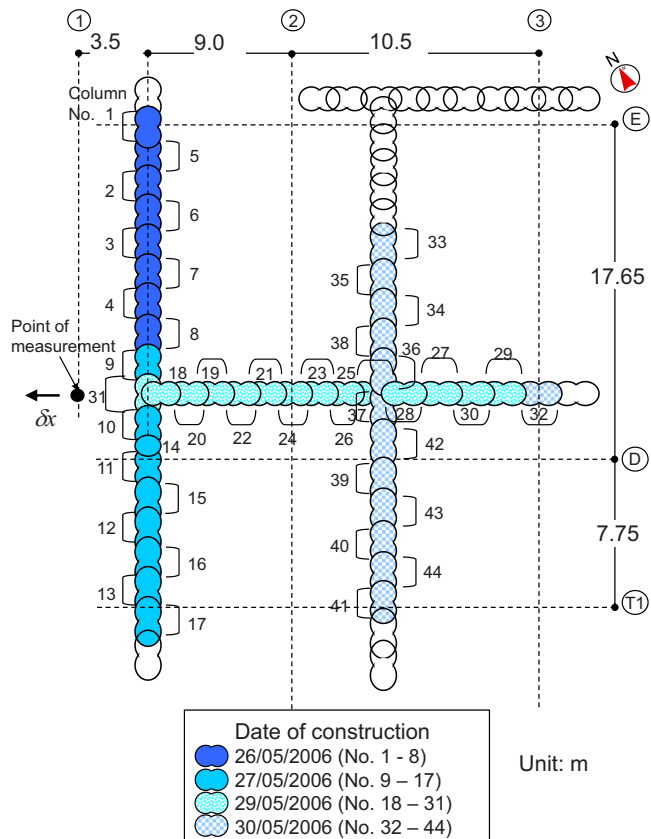


Fig. 14. Plan view of the arrangement of the columns and construction schedule of sandy ground case (data from Minami et al. 2007)

values it was noted that the undrained shear strength of soft clay is typically 10–30 kPa. These parameters were used to calculate the “undrained” shear strength according to the initial effective stress state. For the 1.0 m thick surface crust, a relatively high effective cohesion was assumed to account for its higher strength (and stiffness). Undrained shear strength (S_u) was calculated as follows for all strata except for the silty clay layer:

$$S_u = c' + p_0 \tan \phi' \quad (26)$$

For the silty clay layer S_u was calculated by the equation proposed by Ladd (1991).

Tatsuoka et al. (1986) reported drained strength-deformation characteristics of saturated fine sand under plane strain conditions. For loose fine sand samples with a void ratio (e) of about 0.8, from the representative values of σ'_1/σ'_3 , σ'_3 , and ϵ_a (σ'_1 , σ'_3 are major and minor effective mean stresses, and ϵ_a is vertical strain) at stress levels of 50–75% of the corresponding strength under confining stress of 4.9–98.0 kPa, and assuming an effective stress Poisson ratio $\nu' = 0.3$, the ratios of E'/τ_f (E' is effective stress secant modulus and τ_f is drained strength) of about 100 to 350 can be estimated. The corresponding I_r values are about 38–135. Vesic (1972) suggested that $I_r = 70$ –150 for sand from loose to dense states, and 10–300 for clay from very soft to stiff consistency. Referring to these numbers and considering the fact that the clayey layer at this site is stiffer (and stronger) than soft Ariake clay, the values of Young’s modulus (E) were calculated as 200 times the corresponding S_u values for both sandy and clayey layers. The assumed value of Poisson’s ratio was $\nu = 0.45$ (to allow for some volumetric strain in the elastic region of the soil). With all these parameters, a rigidity index (I_r) of about 68 can be

Table 4. Assumed c' Values and Estimated ϕ' Values from SPT- N Values

Soil layer	Depth (m)	c' or S_u (kPa)	ϕ' (°)
Surface crust	0–1	20	30
Surface layer	1–3	10	30
Clayey sand	3–7	10	25
Fine sand	7–15	2	35
Clayey silt	15–22	10	25
Silty clay	22–30	$0.25\sigma'_{v0}$ ^a	0

^aLadd (1991) for undrained shear strength S_u .

calculated. A value of 68 is almost the lower boundary for sand corresponding to a very loose state as suggested by Vesic (1972). For clay, a value of 68 corresponds to a soft state.

Regarding the radius of the cavity (R_u), no suitable data have been proposed for sandy ground. Since the construction method is CDM, the values listed in Table 3 for CDM were used directly to investigate their applicability to this case. For the pairs of columns designated as Nos. 1–17 and 31, an R_{u0} value of 0.23 m ($E_0 = 2250$ kPa) was evaluated via Eq. (11). Similarly for column Nos. 18–30 and 32–44 a value of 0.2 m was evaluated.

Two calculations of the lateral soil displacements were conducted. One assumed no volumetric strain in the plastic zone ($\Delta = 0$) while the other assumed an average volumetric strain of $\Delta = 4.5\%$ (the back-fitted value) in the plastic zone. The results are compared in Figs. 15(a and b), from which two observations are made.

First, if $\Delta = 0$ is assumed for this sandy ground the calculated displacements are about four times the measured values [Fig. 15(b)], whereas the field data are approximated quite well if $\Delta = 4.5\%$ is assumed. The second observation is that superposition of the lateral displacement is not strictly applicable to cases where subsequent consolidation of the soil causes a considerable reduction in the lateral displacement induced by the cavity expansion. From observations made in the period from May 27 to 29, 2006, superposition generally appears to work well, although on May 27, 2006, the calculated values are larger than the measured data over the depth range 0–10 m, and on May 29, 2006, the calculated displacements are less than the measured data for most depths. However, the lateral displacements of May 30, 2006, calculated using the superposition method, are generally larger than those of May 29, 2006, while the measured data show the reverse tendency [Fig. 15(a)]. Constructing the pair of columns designated as No. 31 caused a large increase in the lateral displacement at the measuring point, and subsequent consolidation (due to dissipation of the excess pore water pressures induced by column installation) appears to have caused a significant reduction in the lateral displacement.

Since the c' values listed in Table 4 were assumed and since a value of $\Delta = 4.5\%$ was back-fitted, the calculation procedure described above is not entirely rigorous. However, there are very few, if any, reported cases of predicting lateral displacements induced by soil-cement column installation in sandy ground, and it is believed that the data presented here may serve as a reference case for future studies of this problem.

Conclusions

A modified method for predicting the lateral displacements in the ground caused by installation of soil-cement columns was pro-

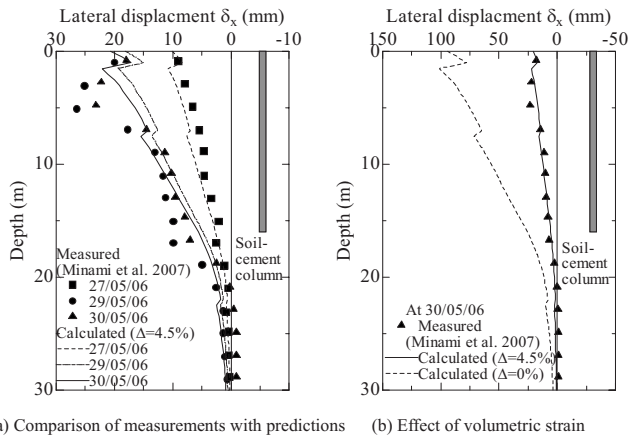


Fig. 15. Comparison of measured and calculated lateral displacements of sandy ground case

posed. The method is a combination of the original method derived by Chai et al. (2005, 2007) based on the theory of cylindrical cavity expansion in an infinite medium, and a correction function to consider the effect of the limited length of the columns. The correction function has been developed by comparing the solutions for a single column installation derived from the theories of spherical and cylindrical cavity expansions.

Both the original and the modified methods have been applied to a case history involving clay soils reported in the literature. By comparing the predicted lateral displacements with the field measurements, the advantage of the modified method over the original method has been demonstrated.

The modified method has also been applied to a case history involving sandy ground. It has been demonstrated that for loose sand the field measurements of lateral displacement can be matched quite well, provided the theoretical method allows volumetric strain to occur in the plastic zone of the soil surrounding the column. For sandy ground this implies that partial drainage can occur and for the case considered, an average volumetric strain of 4.5% was back calculated.

Acknowledgments

The data for the grain-size composition, natural water content, void ratio, and total unit weight profiles shown in Fig. 12, and the grain size distribution curves in Fig. 13 were provided by Dr. E.

Sato of the Takenaka Corporation, Japan. His generous assistance is very much appreciated.

References

- Carter, J. P. (1988). "A semi-analytical solution for swelling around a borehole." *Int. J. Numer. Analyt. Meth. Geomech.*, 12, 197–212.
- Chai, J.-C., Miura, N., and Koga, H. (2005). "Lateral displacement of ground caused by soil-cement column installation." *J. Geotech. Geoenviron. Eng.*, 131(5), 623–632.
- Chai, J.-C., Miura, N., and Koga, H. (2007). "Closure to "Lateral displacement of ground caused by soil-cement column installation." *J. Geotech. Geoenviron. Eng.*, 133(1), 124–126.
- Collins, I. F., and Yu, H. S. (1996). "Undrained expansions of cavities in critical state soils." *Int. J. Numer. Analyt. Meth. Geomech.*, 20(7), 489–516.
- Fujikawa, K., Miura, N., and Beppu, I. (1996). "Field investigation on the settlement of low embankment road due to traffic load and its prediction." *Soils Found.*, 36(4), 147–153 (in Japanese).
- Japanese Society of Civil Engineering. (1986). *Interpretation of the design code for Japanese railway structures*, Earth Pressure Retaining Structures and Foundations, Tokyo, Japan.
- Keer, L. M., Xu, Y., and Luk, V. K. (1998). "Boundary effects in penetration or perforation." *J. Appl. Mech.*, 65, 489–496.
- Ladd, C. C. (1991). "Stability evaluation during staged construction." *J. Geotech. Eng.*, 117(4), 540–615.
- Minami, T., Sato, E., Namikawa, T., and Aoki, M. (2007). "Evaluation of ground deformation during construction of deep mixing method—Part I: Measurement of ground deformation during construction." *Proc., 42th Annual Meeting of Japanese Geotechnical Society*, Japanese Geotechnical Society, Tokyo, Japan, 905–906 (in Japanese).
- Prevost, J. H., and Hoeg, K. (1975). "Analysis of pressure meter in strain softening soil." *J. Geotech. Eng. Div.*, 101(GT8), 717–732.
- Sato, E., Minami, T., Namikawa, T., and Aoki, M. (2007). "Evaluation of ground deformation during construction of deep mixing method—Part II: Effect of deformation control method." *Proc., 42th Annual Meeting of Japanese Geotechnical Society*, Japanese Geotechnical Society, Tokyo, Japan, 907–908 (in Japanese).
- Shen, S. L., Miura, N., and Koga, H. (1999). "Lateral displacement of the surrounding ground during installation of DM columns." *Proceedings of APCOM'99, the 4th Asia-Pacific Conf. on Computational Mechanics*, C. W. Wang, K. H. Lee, and K. K. Ang, eds., Vol. 2, Elsevier Science, New York, 773–778.
- Tatsuoka, F., Sakamoto, M., Kawamura, T., and Fukushima, S. (1986). "Strength and deformation characteristics of sand in plane strain compression at extremely low pressure." *Soil Found.*, 26(1), 65–84.
- Vesic, A. S. (1972). "Expansion of cavities in infinite soil mass." *J. Soil Mech. And Found. Div.*, 98(SM3), 265–290.
- Yu, H. S., and Houlsby, G. T. (1991). "Finite cavity expansion in dilatant soils: Loading analysis." *Geotechnique*, 41(2), 173–183.